CHAPTER 10

SURFACE BEHAVIOUR AND ROTATING RING-DISC ELECTRODE STUDIES OF MoS_xSe_{2-x} ELECTRODES

CONTENTS

10.1 Introduction

It is well known that the photoelectrochemical behaviour of crystalline semiconductor electrodes depends strongly on the surface perfection. This is particularly true for layer type transition metal dichalcogenides, whose performance in photoelectrochemical solar cells has been shown to be extremely sensitive to the crystal surface morphology. It has been observed that the presence of surface steps which act as recombination centers leads to drastic differences in the output characteristics of these photoanodes. Further, faults and steps in particular present on the semiconductor surface act as active sites for corrosion. Therefore, the surface morphology of the semiconductor photoanode not only affects the output characteristics but also the long term performance of the solar cell. In order to evaluate quantitatively the effect of surface morphology on the solar cell performance, a detailed study was carried out on layered transition metal dichalcogenides photoanodes. It may be mentioned that strong influence of the surface morphology on the output characteristics was observed for all TMDC semiconductor surfaces. The present chapter is representative of these observations and deals with studies related to solar cells based on $MoSe_2$ photoanodes.

Successful regenerative operation of a semiconductor-liquid junction solar cell requires no net change in either the electrolyte composition or the semiconductor surface. Thus in an n-type semiconductor, the light separated holes should oxidise the solution species rather than the crystal surface. The resolution of the various reactions paths occuring at photoanodes can therefore be usefully studied with rotating disc electrode (RDE) methodology or the rotating ring-disc electrode (RRDE) technique. This study will provide quantitative and qualitative identification of the various reactants and products formed in photochemical reactions and will also be useful to separate solution processes (e.g.regenerative redox reaction) from surface processes (i.e. photocorrosion). Such photocorrosion studies have been carried out on $MoS_{0.5}Se_{1.5}$, MoSSe and $MoS_{1.5}Se_{0.5}$ and these have also been described in this chapter.

10.2 Results and discussions

Effect of surface morphology and chemical etching on the performance of PEC cells.

In order to study the effect of surface morphology on the performance of the photoanode in the PEC cell, two single crystal surfaces, one with a large number of surface steps (Fig. 10.1(a)) and the other with

a smooth surface (Fig. 10.1(b)) were selected. These were used as photoanodes in the photoelectrochemical cells. Fig. 10.2 (a,b) show the J-V characteristics of the representative cells n-$MoSe_2/I^-$, I_2 (2M, 0.25 M)/Pt with these photoanodes. It is observed that considerable improvement in the short circuit current density, open circuit voltage, fill factor and efficiency for the cell is obtained with smooth surface photoelectrode (Table 10.1). The smooth surface photoelectrode yields a conversion efficiency of 3.43 % which is much higher than that obtained with a stepped surface (0.965 %). The poor performance of the stepped surface is explained as follows.

As even under most careful growing procedure, defects are inevitably present on the van der Waal's surface of layered dichalcogenides as a result of crystal growth processes. Within steps parallel to c-axis, dangling orbitals of both transition metal and chalcogen atoms directly point toward the electrolyte and acts as bonding sites for various species in solution[1)]. The adsorption at and the consequent chemical modification of such sites introduce surface states in the energy gap of the semiconductor which act as traps for photogenerated carriers. Surface steps, grown irregularities and bulk dislocations have recently been identified as recombination centers.

Fig. 10.1 (a,b) SEM photograph of stepped and smooth surfaces of $MoSe_2$ photoanodes respectively.

Fig. 10.2 (a,b) Photocurrent density(J) - Voltage (V) characteristics of stepped and smooth surfaces of $MoSe_2$ photoanodes respectively.

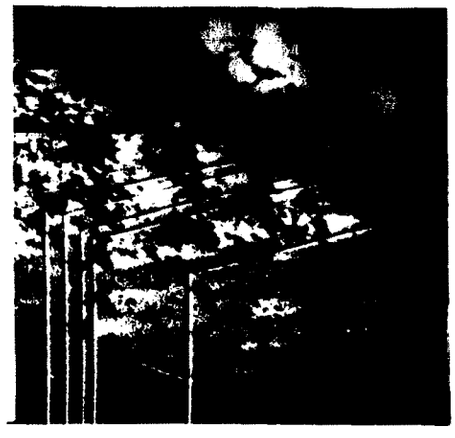

Fig. 10.1(a) X500

Fig. 10.1(b) X500

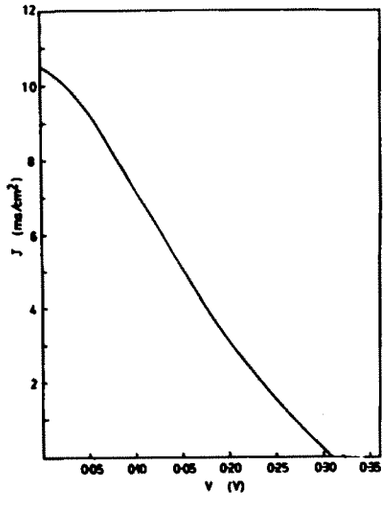

Fig. 10.2(a)

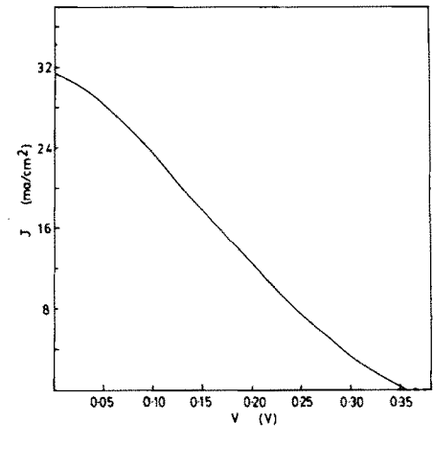

Fig. 10.2(b)

Table 10.1

Performance parameters of PEC cells based on $MoSe_2$ photoelectrodes with smooth and stepped surfaces, before and after chemical etching.

Light intensity = 80 mw/cm^2

$MoSe_2$ photoelectrodes surfaces				
	Smooth		Stepped	
	Prior treatment	Chemical etch	Prior treatment	Chemical etch
Short circuit current I_{sc} (μA)	94	103	74	80
Open circuit voltage V_{oc} (V)	0.358	0.368	0.308	0.321
Fill factor	0.246	0.252	0.239	0.250
Conversion efficiency η (%)	3.430	3.939	0.965	1.143

A possible solution to this problem can be through a specific inhibition or removal of the unsaturated transition metal atoms, by surface treatments with specific chemical agents, which may prevent their interaction with electrolyte. Such type of an approach has been recently attempted by Parkinson et al[2]. In the case of WSe_2 photoanodes long-tailed organic molecules were used to block the recombination centres, but the improvement in performance was only temporary and decayed rapidly during cell operation. Another method used by White et al[3] is the electrochemically initiated polymerization of impervious coating at recombination sites in dark.

During the course of present study, it has been observed that chemical treatment of photoanode surface prior to its use in the cell has profound influence on the performance of the cell. The photoelectrode surfaces were treated chemically in a 2 M solution of chromic acid followed by a treatment in concentrated hydrochloric acid. It is observed that the performance of these photoelectrodes improve after the chemical treatment, for both stepped as well as for smooth surface. The duration of surface treatment in chromic acid and hydrochloric acid was 2 min. and 0.5 min. respectively. The resulting photographs due to chemical treatment for stepped and smooth surfaces are shown in

Fig. 10.3 (a,b) SEM photograph of stepped and smooth surfaces of $MoSe_2$ after chemical treatment respectively.

Fig. 10.4(a, b) Photocurrent (J) - Voltage (V) characteristics of stepped and smooth surfaces of $MoSe_2$ photoelectrode, Curve1, before curve 2, after H_2CrO_4, HCl treatment respectively.

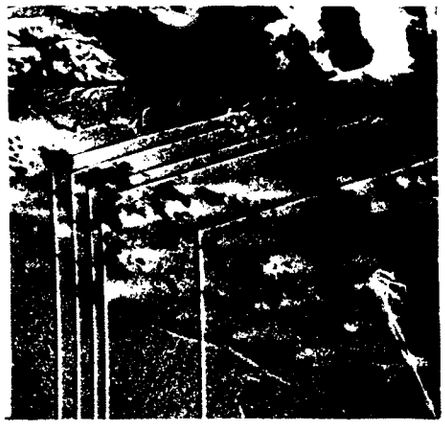

Fig. 10.3(a) X500

Fig. 10.3(b) X500

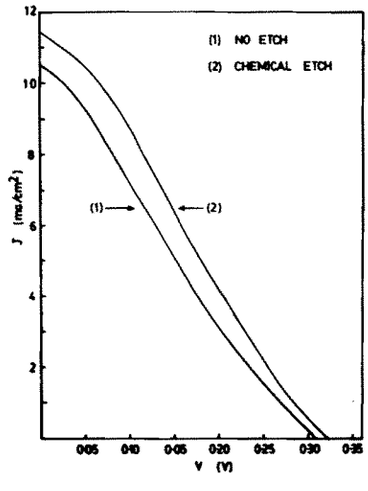

Fig. 10.4(a)

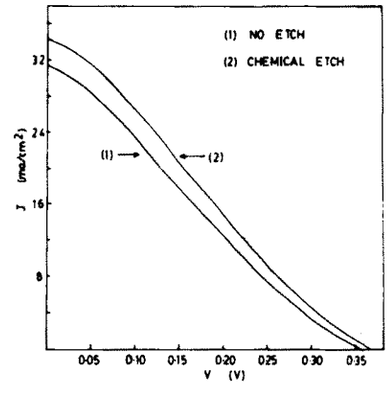

Fig. 10.4(b)

Fig. 10.3 (a and b). The corresponding J-V curves for etched stepped and smooth surface photoelectrodes are shown in Fig. 10.4 (a and b) respectively. The performance parameters of these photoelectrodes before and after treatment are summarized in Table 10.1. Similar observations have been reported by Tenne et al[4] and the improvement in the performance has been attributed to the selective removal of recombination centers from the surface thereby increasing the active surface area of the photoelectrode.

Rotating Ring-Disc Electrode (RRDE) studies on MoS_xSe_{2-x}

The schematic diagram of experimental set up for rotating ring-disc electrode (RRDE) technique[5] is shown in Fig. 10.5, while schematic diagram of the ring-disc electrode is shown in Fig. 10.6. The semiconductor discs were cut from the single crystals of $MoS_{0.5}Se_{1.5}$ MoSSe and $MoS_{1.5}Se_{0.5}$. The ring was made up of platinum wire. The contacts on backside of crystal (disc) were established with silver paste. The backside of crystal and conducting wire leads were insulated using epoxy. The disc and ring were also insulated from each other. The rotating ring disc electrode, which was carefully centered was driven by an electrical motor having 1000 rpm speed. The electrical connections to the electrode system were made directly via

Fig. 10.5 Schematic circuit diagram of rotating ring-disc electrode technique.

Fig. 10.6 Schematic diagram of rotating ring-disc electrode.

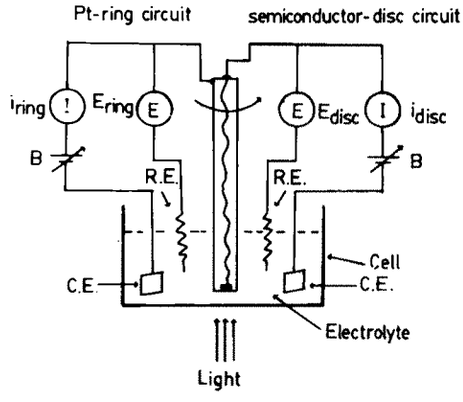

Fig. 10.5

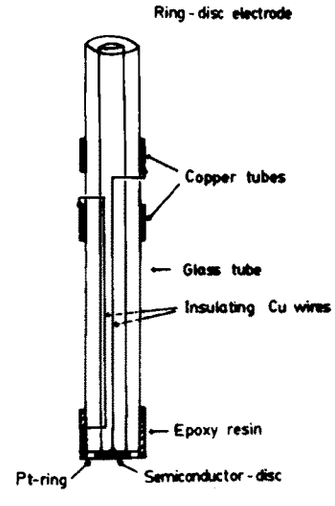

Fig. 10.6

measured from the ring values at zero disc current and at the ring currents plateau at the positive extreme of the disc current. In a similar fashion the changes in ring currents in the cathodic region are due to cathodic reduction of iodine at the disc. In both anodic and cathodic cases the disc current corresponding to ring flux change is related to collection efficiency, N[8]. Ring and disc dimension and current data from Figs. 7(a, b and c) are taculated in Table 10.2 for $MoS_{0.5}Se_{1.5}$, MoSSe and $MoS_{1.5}Se_{0.5}$. The values of N obtained from the geometry and from the values of i_R^+ and i_R^- (Table 10.2) are not identical and thus it is concluded that anodic photo-assisted oxidation of I^- and surface photocorrosion take place simultaneously forming Mo-complex.

10.3 Conclusions

It is observed that the performance of PEC cells based on transition metal dichalcogenides depends upon the surface morphology of photoelectrodes. Performance of cells can be improved by employing the surface pretreatment as chemical etching. Rotating ring-disc electrode studies suggest that the molybdenum sulphoselenides undergo photocorrosion in aqueous iodide/iodine electrolyte.

Fig. 10.7 (a, b and c)

Disc current i_D, ring oxidation current i_R^+ and ring reduction current i_R^-, for $MoS_{0.5}Se_{1.5}$, MoSSe and $MoS_{1.5}Se_{0.5}$ respectively in I^-/I_2 solution under illumination, $E_R^+ = 0.6$ V, $E_R^- = -0.2$ V vs SCE.

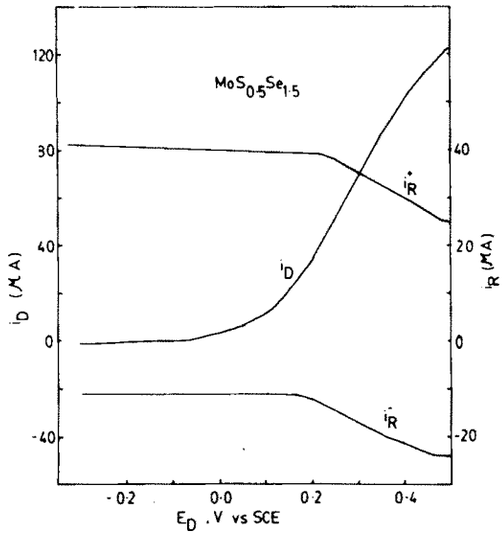

Fig. 10.7(a)

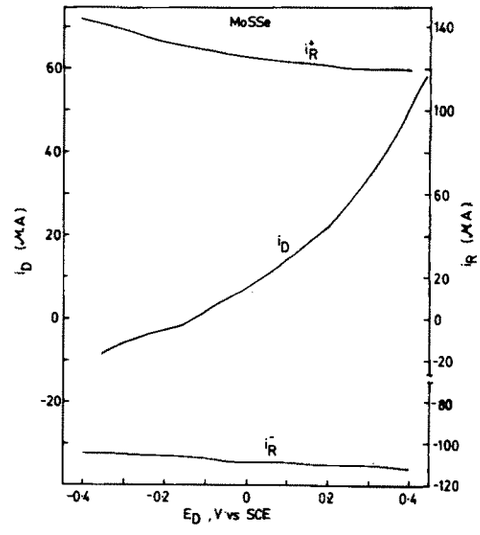

Fig. 10.7(b)

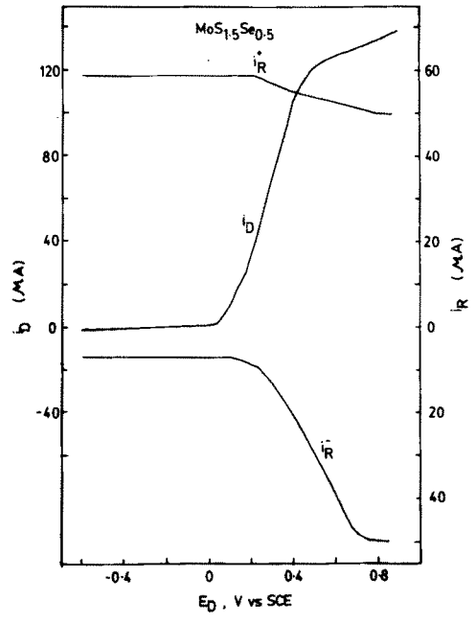

Fig. 10.7(c)

Table 10.2

Ring-disc dimensional and anodic current data from Fig. 7 (a, b, c)

	$MoS_{0.5}Se_{1.5}$	MoSSe	$MoS_{1.5}Se_{0.5}$
Disk radius (cm)	0.124	0.165	0.14
Ring inner radius (cm)	0.134	0.175	0.15
Ring outer radius (cm)	0.184	0.225	0.20
Predicted collection efficiency[8] N	0.4471	0.385	0.415
i_D (μA)	112	52	130
i_R^+ (μA)	15	10	10
i_R^- (μA)	12.5	4	40
N^+	0.1339	0.1923	0.0769
N^-	0.1116	0.0769	0.3076

References

1. Kautek, W., Gobrecht, J. and Gerischer, H. (1980)
Ber. Bunsenges. Phys. Chem. 84, 1034.

2. Parkinson, B. A., Frutak, T. E., Canfield, D., Kam, K. K. and Kline, G. (1981)
Disc. Faraday Soc. 70, 234.

3. White, H. S., Abruna, H. D. and Bard, A. J. (1982)
J. Electrochem. Soc. 129, 2, 265.

4. Tenne, R. and Hodes, G. (1980)
Appl. Phys. Lett. 37, 428.

5. Memming, R. (1977)
Ber. Bunsenges. Phys. Chem. 81, 732.

6. Menezes, S., DiSalvo, F. J. and Miller, B. (1980)
J. Electrochem. Soc. 127, 8, 1751.

7. Ahmed, S. M. (1982)
Electrochimica. Acta. 27, 6, 707.

8. Albery, W. J. and Bruckenstein, S. (1966)
Trans. Faraday Soc. 62, 1920.